

# E2 transitions in the $SU(3)$ formalism for $N = Z$ nuclei of the $sd$ and $pf$ shells

S.M. Lenzi<sup>1,a</sup>, E.E. Maqueda<sup>2,3</sup>, and P. von Brentano<sup>4</sup>

<sup>1</sup> Dipartimento di Fisica, Università degli Studi and INFN, Sezione di Padova, Via F. Marzolo 8, 35131, Padova, Italy

<sup>2</sup> Consejo Nacional de Investigaciones Científicas y Técnicas, Argentina

<sup>3</sup> Departamento de Física, CNEA, Avda. Gral. Paz 1499, (1650) San Martín, Argentina

<sup>4</sup> Institute für Kernphysik, Universität zu Köln, Zùlpicher Straße 77, D-50937 Köln, Germany

Received: 28 October 2005 / Revised version: 23 February 2006 /

Published online: 24 April 2006 – © Società Italiana di Fisica / Springer-Verlag 2006

Communicated by R. Krücken

**Abstract.** We show that the  $SU(3)$  coupling scheme reproduces the data for  $E2$  transitions in  $N = Z$  even-even nuclei both of the  $sd$  and the  $pf$  shells. The  $SU(3)$  results are compared with large-scale shell model calculations. Along the ground-state band-like structures, the increase of the  $B(E2)$  values with spin toward a maximum value and the subsequent fall with further increasing spin are reproduced rather well. The role of the quadrupole-quadrupole term of the nuclear residual interaction is stressed.

**PACS.** 21.60.-n Nuclear-structure models and methods – 21.60.Fw Models based on group theory – 23.20.-g Electromagnetic transitions

## 1 Introduction

Nuclei with equal number of neutrons and protons ( $N = Z$ ) are of particular interest in the study of systems near the limits of stability. A valid question is whether model interpretations developed for light nuclei can be applied to heavier regions.

Such is the case of the models founded on the  $SU(3)$  classification of the many nucleon wave functions [1] that give a microscopic interpretation of the nuclear rotations on the basis of the exact treatment of the quadrupole-quadrupole residual interaction. The  $SU(3)$  scheme was successfully used at the beginning of the  $sd$ -shell within a  $L$ - $S$  coupling. Beyond that region, the spin-orbit force is supposed to have enough influence to break the  $L$ - $S$  coupling and hence, the applicability of the  $SU(3)$  formalism.

A way to check the possible survival of  $SU(3)$  features in heavier regions is to analyze the  $E2$  transitions, given the specificity of the quadrupole operator for the quadrupole-quadrupole interaction, which is proportional to a Casimir operator of the  $SU(3)$  group of symmetries.

Since the first applications of the  $SU(3)$  picture to nuclear spectroscopy [2] many authors have dealt with the analysis of the  $E2$  transitions in relation to that framework. In most cases the calculations implied the solution in bases classified by the irreps of the  $SU(3)$  group of

schematic or realistic Hamiltonians, which meant, in practice, departures from the pure  $SU(3)$ . There are some recent references [3,4] in which this subject is addressed for even-even nuclei of the  $sd$  and  $pf$  shells, respectively.

In ref. [3] a quasi- $SU(3)$  truncation scheme is used in conjunction with a Hamiltonian that includes Nilsson single-particle, quadrupole-quadrupole, pairing and rotor-like terms to calculate  $B(E2)$  transition strengths.

Relative  $B(E2)$  values are obtained in ref. [4] within a shell model calculation with a realistic Kuo-Brown interaction in a full  $pf$  space. They compare results obtained with realistic single-particle splittings and degenerate  $p$  and  $f$  shells as well as the predictions for the  $SU(3)$  limit.

In the present work we calculate the  $B(E2)$  values for rotational-like structures based on the ground state of a number of  $N = Z$  systems in the  $sd$  and  $pf$  shells. The formalism in the pure  $SU(3)$  scheme, approximate treatments and the calculations that support the method are introduced in sect. 2. The results are shown in sect. 3 and compared with data. The final remarks are given in sect. 4.

## 2 Formulas and method

### 2.1 The pure $SU(3)$ scheme

The quadratic Casimir operators of  $SU(3)$  can be written in terms of a quadrupole-quadrupole and a rotational

<sup>a</sup> e-mail: lenzi@pd.infn.it

term,

$$C_2 = (\mathbf{Q} \cdot \mathbf{Q}) + 3(\mathbf{L} \cdot \mathbf{L}), \quad (1)$$

which implies that in a basis classified by  $SU(3) \supset \mathcal{R}(3)$ , a Hamiltonian with a two-body term proportional to a quadrupole-quadrupole interaction,

$$H = H_{sp} + \kappa(\mathbf{Q} \cdot \mathbf{Q}), \quad (2)$$

results diagonal. Since the  $E2$  transition operator is proportional to  $Q$ , *i.e.*,

$$\mathcal{M}(E2) = \frac{1}{2}(e_\pi + e_\nu) \frac{\hbar}{M\omega} \sqrt{\frac{5}{16\pi}} \mathbf{Q}, \quad (3)$$

and this is one of the generators of  $SU(3)$ , is therefore natural to use the  $E2$  transitions as probes of the adequacy of the use of the irreducible representations of this group for the classification of the states describing a given nuclear system.

We calculate the  $B(E2)$  values in  $N = Z$  nuclei where we expect that the  $SU(3)$  behavior has not been blurred out by the spin-orbit interaction. That is the case of  $E2$  transitions in the ground-state bands of the even-even  $N = Z$  nuclei  $^{20}\text{Ne}$ ,  $^{24}\text{Mg}$ ,  $^{28}\text{Si}$ ,  $^{44}\text{Ti}$ , and  $^{48}\text{Cr}$ . We assume that the yrast band of this nuclei correspond to states belonging to the highest orbital symmetry (labelled by the partition  $[f]$  of the number of nucleons) and the leading representation  $(\lambda, \mu)$  of the  $SU(3)$  group, namely,

$^{20}\text{Ne}$ :	$[4](8, 0)$
$^{24}\text{Mg}$ :	$[44](8, 4)$
$^{28}\text{Si}$ :	$[444](12, 0)$
$^{44}\text{Ti}$ :	$[4](12, 0)$
$^{48}\text{Cr}$ :	$[44](16, 4)$

The classification of states according to irreducible representations of the symmetric and  $SU(3)$  Groups is explained in ref. [1]. In particular, tables 1 and 2 of that reference contain the classification of states in the  $N = 2$  and  $N = 3$  oscillator shell. We give more details of the significance of this classification in sect. 2.4.

All members of a  $[f](\lambda, \mu)$ -band are built from the same intrinsic structure. The intrinsic ( $\chi$ ) and laboratory ( $\psi$ ) functions are related by

$$\psi((\lambda, \mu)KLM) = \frac{(2L+1)}{\sqrt{A((\lambda, \mu)K L K)}} \int \mathcal{D}_{MK}^L(\Omega) \chi_\Omega(\lambda, \mu) d\Omega \quad (4)$$

and its inverse,

$$\chi(\lambda, \mu) = \sum_{K,L} \sqrt{A((\lambda, \mu)K L K)} \psi((\lambda, \mu)K L K). \quad (5)$$

The  $SU(3)$  normalization constant can be cast as

$$A((\lambda, \mu)K L K') = \frac{(2L+1)}{8\pi^2} \sum_{n=0}^{\mu} \frac{(-1)^n \mu!}{n!(\mu-n)!} \times \left\{ \int_0^{2\pi} d\alpha e^{iK'\alpha} \sin \alpha^n \cos \alpha^{\mu-n} \right\}$$

$$\times \left\{ \int_0^{2\pi} d\gamma e^{iK\gamma} \sin \gamma^n \cos \gamma^{\mu-n} \right\} \times \left\{ \int_{-1}^{+1} d \cos \beta \cos \beta^{\lambda+n} d_{K',K}^L(\beta) \right\}. \quad (6)$$

The quadrupole operator, being a generator of  $SU(3)$ , does not connect states belonging to different representations of the group. The matrix element  $\langle(\lambda, \mu)K'L' \| Q \| (\lambda, \mu)KL\rangle$ , entering in the calculation of the  $B(E2)$  values, can be obtained by resorting to tables [5] or computer codes [6] that give  $SU(3) \supset R(3)$  Wigner coefficients. For the sake of self-contention, we prefer to use the simple original  $SU(3)$  expressions [7]. The quadrupole matrix element is given by

$$\begin{aligned} \langle(\lambda, \mu)K'L' \| Q \| (\lambda, \mu)KL\rangle &= \frac{2L+1}{\sqrt{2L'+1}} \\ &\times \left[ \langle LK20 | L'K' \rangle \sqrt{\frac{A((\lambda, \mu)K L' K')}{A((\lambda, \mu)K L K)}} \langle(\lambda, \mu)L'K' | (\lambda, \mu)L'K' \rangle \right. \\ &\times \left. \left\{ \begin{array}{c} 2\lambda + \mu + \frac{1}{2}(L'(L'+1) + 6 - L(L+1)) \\ -2\mu - \lambda - \frac{1}{2}(L'(L'+1) + 6 - L(L+1)) \end{array} \right\} \right. \\ &+ \sum_{\pm} \langle LK2 \pm 2 | L'K' \pm 2 \rangle \sqrt{\frac{3(\mu \mp K)(\mu \pm K + 2)}{2}} \\ &\times \frac{b((\lambda, \mu)K)}{b((\lambda, \mu)K \pm 2)} \sqrt{\frac{A((\lambda, \mu)K \pm 2L'K \pm 2)}{A((\lambda, \mu)K L K)}} \\ &\left. \times \langle(\lambda, \mu)L'K' | (\lambda, \mu)L'K' \pm 2 \rangle \right] \quad (7) \end{aligned}$$

(in the curly bracket, the upper value applies to  $\lambda \geq \mu$  and the lower to  $\lambda < \mu$ ). The coefficients  $b((\lambda, \mu)K)$  transform from the Cartesian to the  $K$ -defined basis. We remind that the  $SU(3)$  wave functions for different  $K$ 's are not orthogonal and the overlaps are calculated as

$$\langle(\lambda, \mu)LK' | (\lambda, \mu)LK\rangle = \frac{A((\lambda, \mu)K L K')}{\sqrt{A((\lambda, \mu)K L K)A((\lambda, \mu)K' L K')}}. \quad (8)$$

With the above formulae the values of  $B(E2)$  in  $e^2 \text{fm}^4$  are obtained.

## 2.2 Axial alignment and rigid rotation

If all the quanta were to align along one intrinsic axis (*i.e.*, the  $z$ -axis) the  $SU(3)$  states of a nucleus with  $k$  valence particles would have  $(\tilde{\lambda}, \tilde{\mu}) = (kN, 0)$  ( $N$ : shell quantum number). In general, charge and spin restrict the number of particles that can align quanta in a given direction, which implies  $\lambda \leq \tilde{\lambda}$  and —depending of the particle number—  $\mu \neq 0$ . In the case of the nuclei of our interest, *i.e.*  $^{20}\text{Ne}$ ,  $^{24}\text{Mg}$ ,  $^{28}\text{Si}$ ,  $^{44}\text{Ti}$ , and  $^{48}\text{Cr}$ , no restriction on the number of quanta in the symmetry axis would imply  $(\tilde{\lambda}, \tilde{\mu})$  equal to  $(8, 0)$ ,  $(16, 0)$ ,  $(24, 0)$ ,  $(12, 0)$ , and  $(24, 0)$ ,

instead of the respective  $(8, 0)$ ,  $(8, 4)$ ,  $(12, 0)$ ,  $(12, 0)$ , and  $(16, 4)$  (for four valence nucleons ( $^{20}\text{Ne}$  and  $^{44}\text{Ti}$ ) the values of  $(\lambda, \mu)$  remain the same). For the above “stretched  $SU(3)$ ” states the normalization constant of eq. (6) can be calculated to be

$$A((\tilde{\lambda}, \tilde{\mu} = 0), K = 0, L, K' = 0) = \frac{2^{(L-\tilde{\lambda})/2} \tilde{\lambda}!}{\left(\frac{\tilde{\lambda}-L}{2}\right)! (\tilde{\lambda} + L + 1)!!}. \quad (9)$$

Taking this expression into eq. (7) we can obtain the corresponding  $E2$  matrix element for stretched states. In the case of an  $E2$  transition  $J + 2 \rightarrow J$  results in

$$\langle(\tilde{\lambda}, 0)0(J-2)\|Q\|(\tilde{\lambda}, 0)0J\rangle = 2\langle J020|(J-2)0\rangle \times \sqrt{(2J+1)(\tilde{\lambda}+J+1)(\tilde{\lambda}-J+2)}. \quad (10)$$

This expression has been related to the  $SU(3)$  symmetry in ref. [8] and is valid for boson approximations. In order to appreciate the effects of the full consideration of antisymmetry we compare the results of this “stretched  $SU(3)$ ” (eq. (10)) with those obtained for a fermionic  $SU(3)$  using eq. (7).

For  $\lambda \rightarrow \infty$  the  $SU(3)$  intrinsic wave function is totally peaked in the  $z$ -direction and the wave function (eq. (4)) becomes that of a rigid rotor ( $\psi((\lambda, \mu)KLM) \propto \chi \mathcal{D}_{MK}^L$ ). In this case the quadrupole transition matrix element is

$$\langle 0(J-2)\|Q\|0J\rangle = \langle J020|(J-2)0\rangle \sqrt{(2J+1)} Q_0, \quad (11)$$

with  $Q_0$  an overall constant independent of  $J$ .

In sect. 4 we discuss the differences that eqs. (7), (10) and (11) make in the behavior of the  $B(E2)$ 's as functions of nuclear spins, specially for large values of  $J$ .

### 2.3 Mixing of $SU(3)$ configurations

As can be seen from eq. (1), in states classified by the irreps of the  $SU(3)$  group (labelled by  $(\lambda, \mu)$ ), the energies corresponding to a quadrupole-quadrupole Hamiltonian and no single-particle splitting depend, apart from the rotational  $L(L+1)$  term, solely on the eigenvalues of the Casimir operator  $C_2$ , which is expressed in terms of the values of  $\lambda$  and  $\mu$  as

$$\langle C_2 \rangle = 4(\lambda^2 + \mu^2 + \lambda\mu + 3\lambda + 3\mu). \quad (12)$$

From this expression some  $(\lambda, \mu)$  or  $K$  degeneracies result in the case of the nuclei under consideration. The interactions left out of the simple model Hamiltonian indicated above are responsible for the splitting of the levels and mix the degenerate configurations. A calculation of the mixing of configurations by solving the residual force is outside the scope of the present paper. Nevertheless, considering the importance that such a mixing could have in the final result we make some schematic assumptions to take it into account. Two different sources of degeneracies are considered in the following. In both cases we assume that the mixing of the  $SU(3)$  configurations stems from the mixing of the intrinsic states  $\chi(\lambda, \mu)$ .

#### 2.3.1 $(\lambda, \mu)$ degeneracy

In the case of  $^{28}\text{Si}$  there are two representations  $[(12, 0)$  and  $(0, 12)]$  that come lowest in energy since they have the same eigenvalue of  $C_2$ . We can then expect that the intrinsic state on which the yrast band is built would result a combination of the two representations. The calculation of the  $B(E2)$  values in the  $SU(3)$  scheme will, therefore, imply the determination of the mixture of those two configurations.

#### 2.3.2 $K$ degeneracy

In the  $SU(3)$  scheme, if  $\mu > 0$ , there are more than one  $K$  state belonging to the same irrep,  $K = \mu, \mu-2, \dots, 1$  or  $0$ . These states are also degenerate, as results from eqs. (1) and (12). In our case this degeneracy can occur for the nuclei  $^{24}\text{Mg}$  and  $^{48}\text{Cr}$ .

In a treatment as in ref. [2], in which any central interaction can be expressed in terms of angular-momentum operators acting on the intrinsic  $SU(3)$  leading states, we can assume that the  $K$ -mixing comes from an  $L_{+1}^2 + L_{-1}^2$  term which can be considered as a perturbation. The result is a mixing of  $K = 2$  states in the  $K = 0$  ground-state band ( $J \neq 0$ ),

$$\Psi((\lambda, \mu)J, M) \propto \psi((\lambda, \mu)K = 0, J, M) + \epsilon \psi((\lambda, \mu)K = 2, J, M), \quad (13)$$

where  $\epsilon$  does not depend on  $J$ . Although calculations with a realistic force [2] show that the  $K$ -mixing, even if small, increases with the angular momentum  $J$ , the use of  $J$ -dependent mixing coefficients in (13), arising from more general perturbations would mean, within the simple philosophy of the present treatment, the introduction of too many parameters.

### 2.4 About the influence of the spin-orbit term

The applicability of the  $SU(3)$  formalism depends on the possibility of neglecting the spin-orbit interaction. For  $N = Z$  even-even nuclei the attractive part of the potential brings lowest the states of highest orbital symmetries, which in the case of these nuclei belong to the partitions  $[44 \dots 4]$ . To form an antisymmetric state the spin-isospin part of the function must belong to the conjugated symmetry  $[\widetilde{44 \dots 4}]$  for which, since  $T = 0$ , it must be  $S = 0^1$ . For such states the spin-orbit force gives no first-order effect [2]. The states that can be mixed by the spin-orbit interaction belong to orbital symmetries  $[44 \dots 31]$ , which in first order are well apart in energy from those belonging to the highest orbital symmetry. Hence, if no spin-orbit force is active, the states of the yrast band will belong only to the orbital symmetry  $[44 \dots 4]$ , or conversely, if the spin-orbit force is relevant, the wave functions of the

<sup>1</sup> A justification of this assumption in terms of group theory can be found, for example, in refs. [9–11].

states under consideration will have contributions of orbital symmetries [4...31] or lower.

The  $M1$  operator,

$$\mathcal{M}(M1) = \left(\frac{3}{4\pi}\right)^{\frac{1}{2}} \frac{e\hbar}{2Mc} (g_l \mathbf{l} + g_s \mathbf{s}) \quad (14)$$

can be considered specific for the spin-orbit interaction  $\mathbf{l}\cdot\mathbf{s}$ . We can, therefore, measure the sensibility of neglecting the spin-orbit part of the nuclear force for the description of the bands under consideration by assessing the amount of  $M1$  relating states of these bands to other nearby states thought to belong to the same [44...4] orbital symmetry. In fact, as we will show in the following, we find that all such  $M1$ 's are very small.

We analyze the transitions populating the first  $2_1^+$  states from the second  $2_2^+$  states in the nuclei of interest. To appraise the magnitude of the corresponding value of  $B(M1)$  we compare it to the respective values for transitions in nearby nuclei for which the spin-orbit term is expected to be relevant. That is the case of  $M1$  transitions in an adjoining odd-even nucleus relating presumed single-particle states or  $M1$  transitions in even-even nucleus differing in two nucleons ( $|N-Z|=2$ ), for which the lowest states belong to the orbital symmetry [44...2] that allows  $S=1$  components. The mixing ratios  $\delta(E2/M1)$  are also quoted in the cases that are known.

#### $^{20}\text{Ne}$

$^{20}\text{Ne}$ ,  $2_2^+ \rightarrow 2_1^+$ :  
 $B(M1; E_\gamma = 5.787 \text{ MeV}) = 1.0(3) \cdot 10^{-4} \text{ W.u.}$ ,  $\delta = 8.4_{-10}^{+15}$ ,  
 while in  $^{21}\text{Ne}$ ,  $7_2^+ \rightarrow 5_2^+$ :  
 $B(M1; E_\gamma = 1.396 \text{ MeV}) = 0.145(9) \text{ W.u.}$ ,  $\delta = -0.14(2)$   
 and in  $^{22}\text{Ne}$  (the lowest symmetry is [42]),  $2_2^+ \rightarrow 2_1^+$ :  
 $B(M1; E_\gamma = 3.181 \text{ MeV}) = 1.8(3) \cdot 10^{-2} \text{ W.u.}$ ,  $\delta = -9(2) \cdot 10^{-2}$ .

#### $^{24}\text{Mg}$

$^{24}\text{Mg}$ ,  $2_2^+ \rightarrow 2_1^+$ :  
 $B(M1; E_\gamma = 2.869 \text{ MeV}) = 7.7 \cdot 10^{-6} \text{ W.u.}$ ,  $\delta = 23(9)$ ,  
 while in  $^{25}\text{Mg}$ ,  $3_2^+ \rightarrow 1_2^+$ :  
 $B(M1; E_\gamma = 0.390 \text{ MeV}) = 1.59(6) \cdot 10^{-2} \text{ W.u.}$ ,  $\delta = 0.13(3)$ ,  
 and in  $^{26}\text{Mg}$  (the lowest symmetry is [442]),  $2_2^+ \rightarrow 2_1^+$ :  
 $B(M1; E_\gamma = 1.130 \text{ MeV}) = 9.7(1.2) \cdot 10^{-2} \text{ W.u.}$ ,  $\delta = -0.12(2)$ .

#### $^{28}\text{Si}$

$^{28}\text{Si}$ ,  $3^+ \rightarrow 2^+$ :  
 $B(M1; E_\gamma = 4.496 \text{ MeV}) = 2.5(2) \cdot 10^{-4} \text{ W.u.}$   $\delta = -0.14(2)$ ,  
 while in  $^{29}\text{Si}$ ,  $3_2^+ \rightarrow 1_2^+$ :

$B(M1; E_\gamma = 1.273 \text{ MeV}) = 3.5(2) \cdot 10^{-2} \text{ W.u.}$ ,  $\delta = 0.197(9)$ ,  
 and in  $^{30}\text{Si}$  (the lowest symmetry is [4442]),  $2_2^+ \rightarrow 2_1^+$ :  
 $B(M1; E_\gamma = 1.263 \text{ MeV}) = 9.4(9) \cdot 10^{-2} \text{ W.u.}$ ,  $\delta = 0.18(4)$ .

#### $^{44}\text{Ti}$

$^{44}\text{Ti}$ ,  $2_2^+ \rightarrow 2_1^+$ :  
 $B(M1; E_\gamma = 1.448 \text{ MeV}) = 8(7) \cdot 10^{-5} \text{ W.u.}$ ,  $\delta = -8_{-8}^{+3}$ ,  
 while in  $^{45}\text{Ti}$ ,  $5_2^- \rightarrow 7_2^-$ :  
 $B(M1; E_\gamma = 0.040 \text{ MeV}) = 2.27(9) \cdot 10^{-3} \text{ W.u.}$ ,  $\delta = 0.000(25)$ ,  
 and in  $^{46}\text{Ti}$  (the lowest symmetry is [42]),  $2_2^+ \rightarrow 2_1^+$ :  
 $B(M1; E_\gamma = 2.073 \text{ MeV}) = 5.8(9) \cdot 10^{-3} \text{ W.u.}$ ,  $\delta = -1.21(14)$ .

#### $^{48}\text{Cr}$

$^{48}\text{Cr}$ : no lifetimes available for transitions feeding the  $2_1^+$ .

### 3 The results

Figures 1 to 5 show the  $B(E2)$  data for transitions within the ground-state bands in the nuclei  $^{20}\text{Ne}$ ,  $^{24}\text{Mg}$ ,  $^{28}\text{Si}$ ,  $^{44}\text{Ti}$ , and  $^{48}\text{Cr}$ , respectively. The same figures display the results of the calculations in the  $SU(3)$  scheme and of the shell model. This latter model has achieved very good agreement with the spectroscopic data, both in the  $sd$  and  $pf$  shells. We will, therefore, use its results as a paragon for comparison with other model calculations as the present one. To obtain the shell model  $B(E2)$  values we have used the code ANTOINE [12]. For  $sd$ -shell nuclei the USD effective interaction [13] in the full  $sd$  space has been used, while, for  $pf$ -shell nuclei we have adopted the KB3G interaction [14] in the full  $pf$  valence space. In the cases of  $N=Z$  nuclei, the sum of the effective charge ( $e_\pi + e_\nu$ )

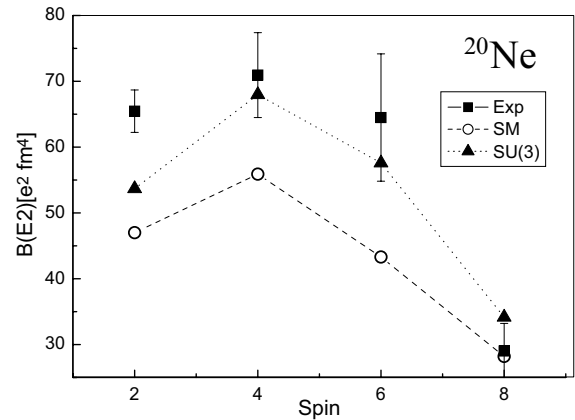


**Fig. 1.** Experimental (Exp) [15], shell model (SM) and  $SU(3)$   $B(E2)$  values as a function of the initial spins for the ground-state band in  $^{20}\text{Ne}$ .

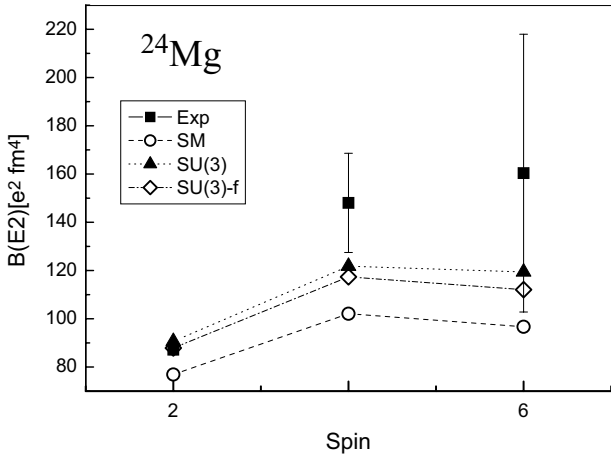


**Fig. 2.** Experimental (Exp) [16], shell model (SM),  $SU(3)$  and best fit allowing  $K$ -mixing perturbation ( $SU(3)$ -f)  $B(E2)$  values as a function of the initial spins for the ground-state band in  $^{24}\text{Mg}$ .

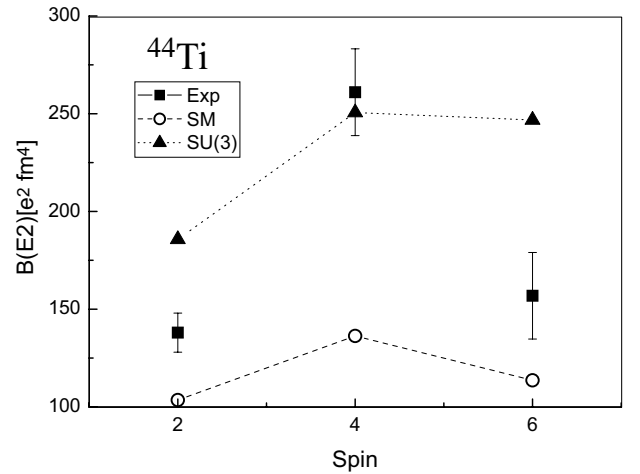


**Fig. 4.** Experimental (Exp) [17], shell model (SM) and  $SU(3)$   $B(E2)$  values as a function of the initial spins for the ground-state band in  $^{44}\text{Ti}$ .

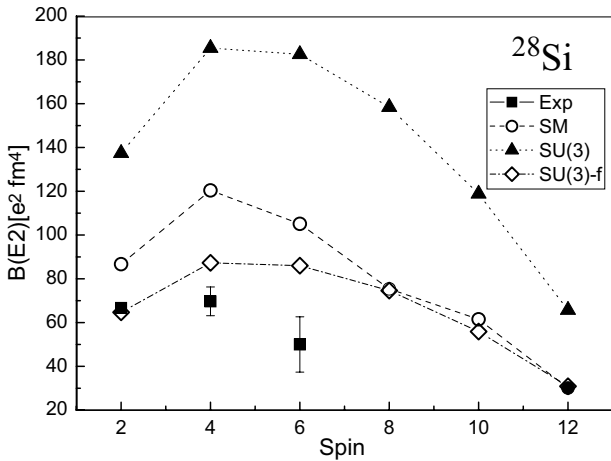


**Fig. 3.** Experimental (Exp) [16], shell model (SM),  $SU(3)$  and best fit allowing  $K$ -mixing perturbation ( $SU(3)$ -f)  $B(E2)$  values as a function of the initial spins for the ground-state band in  $^{28}\text{Si}$ .

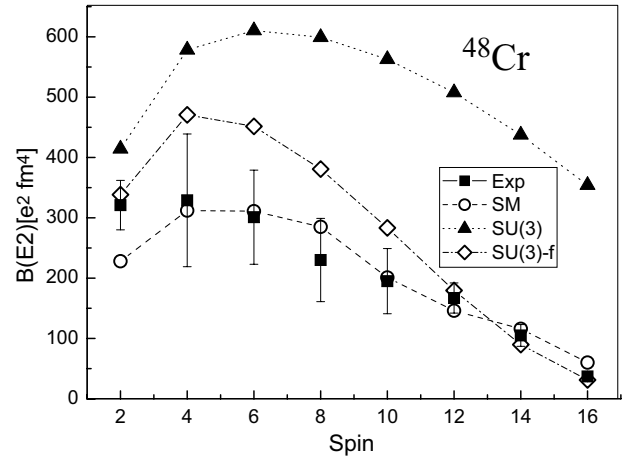


**Fig. 5.** Experimental (Exp) [18], shell model (SM),  $SU(3)$  and best fit allowing  $K$ -mixing perturbation ( $SU(3)$ -f)  $B(E2)$  values as a function of the initial spins for the ground-state band in  $^{48}\text{Cr}$ .

enters as an overall scaling factor in the calculation of  $B(E2)$ . For the effective charges we have used  $e_\pi = 1.5$  and  $e_\nu = 0.5$  in both shells. In shell model calculations these values reproduce well the spectroscopy of  $f_{7/2}$ -shell nuclei while in the  $sd$ -shell, nuclear-mass-dependent values produce better agreement.

$^{20}\text{Ne}$ : this is a nucleus where  $SU(3)$  is known to work properly. In fact, fig. 1 shows a very good agreement with the data of the  $SU(3)$  predictions. Although the shell model reproduces the behavior of the values of  $B(E2)$  as function of the angular momenta, the  $B(E2)$  values are underestimated. To get a better agreement with data, the effective charges used in the shell model calculation should be increased by 10–15%.

$^{24}\text{Mg}$ : the  $SU(3)$  formalism reproduces properly the magnitude of the three experimental points in fig. 2. Allowing the action of a  $K$ -mixing perturbation (sect. 2.3.2) does not improve greatly the quality of the agreement with the data, which is implied by the fact that the best fit is obtained for a very small perturbation ( $\epsilon = 0.03$ ). As in the case of  $^{20}\text{Ne}$  an increase of the effective charges could allow a better shell model description of the data.

$^{28}\text{Si}$ : the calculation of the  $B(E2)$  values for only one irrep of  $SU(3)$ , corresponding to the lowest energies (either (12, 0) or (0, 12)) overestimates the transition strengths in fig. 3. From sect. 2.3.1 we can expect a mixing of the “oblate”[(0, 12)] and “prolate”[(12, 0)]  $SU(3)$  configurations. Experimental evidence of shape coexistence in this nucleus [19] supports this assumption. The quadrupole reduced matrix elements corresponding to the two  $(\lambda, \mu)$  representations are equal and of opposite sign, therefore,

they will contribute destructively to the  $B(E2)$  value, a fact that results crucial to get the right magnitude. A general interaction can mix two  $(\lambda, \mu)$  configurations, provided that their eigenvalues of  $Q_0$  and  $(Q_2 + Q_{-2})/\sqrt{6}$  differ in less than  $6N$  and  $4N$ , respectively [2]. In the case of  $^{28}\text{Si}$ , where  $N = 2$ , the states belonging to the  $(12, 0)$  and  $(0, 12)$  representations cannot be directly connected, since the difference of the second of the above eigenvalues is  $12 > 8$ . The amount of admixture (19%) needed to achieve the best fit can be justified as a second-order process facilitated by the degeneracy of the zeroth-order energies. This mixing, as well, is the responsible of the sizable  $E2$  transitions from the excited  $0^+$  states to the yrast  $2^+$  state. Using these experimental  $B(E2)$  values, it is straightforward to obtain a mixing which is consistent with that of the best fit. To have a better shell model description of the data, *smaller* effective charges would be needed.

$^{44}\text{Ti}$ : in this case we cannot draw conclusions about the comparative quality of the results either of the  $SU(3)$  or of the shell model calculations: although both give the right order of magnitude, they fail to reproduce the abrupt fall for the  $6^+ \rightarrow 4^+$  transition (see fig. 4). It is important to note that the first two transitions  $2^+ \rightarrow 0^+$  and  $4^+ \rightarrow 2^+$  have been recently measured [17], while there is not new data for the transition  $6^+ \rightarrow 4^+$ .

$^{48}\text{Cr}$ : this is a nucleus where the large-scale shell model has been particularly successful in reproducing the spectroscopic data. The  $SU(3)$  results, for a pure  $(\lambda, \mu) = (16, 4)$ ,  $K = 0$  configuration overestimate the data in fig. 5. A sensible fit is achieved by mixing the  $K = 2$  band, along the line of sect. 2.3.2, with  $\epsilon = 0.19$ .

## 4 Final remarks

We have been able to obtain a rather good fit to the  $B(E2)$  experimental values for  $sd$  and  $pf$  nuclei using the  $SU(3)$  formalism with the same effective charges in all cases.

The above indication in favor of considering, based on such a simple picture, the  $SU(3)$  as a good symmetry for these nuclei contradicts—or better, concludes differently than—analyses mainly aimed at reproducing the energy spectra. The explanation can be found in the fact that, for the  $N = Z$  even-even nuclei, the nuclear states are strongly dominated by the  $\mathbf{Q} : \mathbf{Q}$  component of the interaction (see, for example, ref. [20]) while energies may depend on subtle components of the interaction or on terms that do not modify the  $E2$  transition rates.

We note that not only the increase of the  $B(E2)$  values with spin toward a maximum but also the subsequent decrease to very small values with further increasing spin is reproduced rather well. Although the  $SU(3)$  is the right microscopic interpretation of the nuclear rotations, its results differ from a stretched picture (eq. (10)) and from a rigid rotator (eq. (11)). For the sake of comparison, in fig. 6

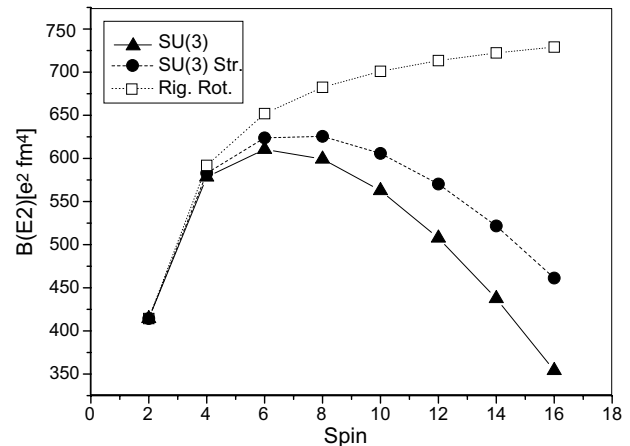


**Fig. 6.**  $B(E2)$  values as a function of the initial spins for  $SU(3)((\lambda, \mu) = (16, 4))$  (full triangles), a stretched  $SU(3)((\lambda, \tilde{\mu}) = (24, 0))$  (full circles), and a rigid rotator (open squares). Values are normalized to the first  $SU(3)$  value. The parameters  $(\lambda, \mu)$  (or  $(\tilde{\lambda}, \tilde{\mu})$ ) have been chosen to correspond to  $^{48}\text{Cr}$ .

we show the results corresponding to  $SU(3)$ , a stretched  $SU(3)$ , and a rigid rotator.

The appropriate behavior of  $SU(3)$  in reproducing the data tendency as a function of the spin is associated to its right consideration of the interplay of the nuclear-states collectivity, the full symmetries and the finite size of the shells.

Even though the fit is best for the lighter of the considered nuclei,  $^{20}\text{Ne}$ , nevertheless we obtain good results for the  $pf$  nuclei despite the *a priori* large single-particle splitting operating in this major shell.

We confirm therefore the hypothesis that for those states for which an  $L$ - $S$  coupling is valid, that is, in which the effect of the spin-orbit results nullified by symmetry reasons, the mixing of configurations that sustains irreps of  $SU(3)$  gives a good description of the states of the yrast band, as regards to quadrupole transitions. We show that this is the case in g.s. band-like structures of even-even  $N = Z$  nuclei of the  $sd$  and  $pf$  shells.

The authors would like to thank A. Vitturi for fruitful and interesting discussions. This work was partially supported by PIP 02618 of CONICET, Argentina.

## References

1. J.P. Elliott, Proc. R. Soc. London, Ser. A **245**, 128; 562 (1958).
2. J.P. Elliott, M. Harvey, Proc. R. Soc. London, Ser. A **272**, 557 (1963).
3. C.E. Vargas, J.G. Hirsch, J.P. Draayer, Nucl. Phys. A **690**, 409 (2001).
4. V.G. Gueorguiev, J.P. Draayer, C.W. Johnson, Phys. Rev. C **63**, 014318 (2000).
5. J.D. Vergados, Nucl. Phys. A **111**, 681 (1968).
6. Y. Akiyama, J.P. Draayer, Comput. Phys. Commun. **5**, 405 (1973).

7. M. Harvey, in *Advances in Nuclear Physics*, edited by M. Baranger, E. Vogt, Vol. **1** (Plenum Press, New York, 1968) p. 67.
8. A. Bohr, B. Mottelson, *Nuclear Structure*, Vol. **II** (Benjamin, New York, 1975) p. 94.
9. J.P. Elliott, P.G. Dawber, *Symmetry in Physics*, Vol. **2** (Oxford University Press, New York, 1979) Chaps. 17 and 18.
10. J.P. Elliott, A.M. Lane, *Handbuch der Physik*, edited by S. Flugge, Vol. **39** (Springer, Berlin, 1957) Sect. 18.
11. M. Hammermesh, *Group Theory and its Application to Physical Problems* (Addison-Wesley Publishing Company, Inc., Reading, Mass., 1962) Sect. 11-7.
12. E. Caurier, F. Nowacki, *Acta Phys. Pol.* **30**, 705 (1999).
13. B.A. Brown, B.H. Wildenthal, *Annu. Rev. Nucl. Part. Sci.* **38**, 29 (1988).
14. A. Poves, J. Sánchez-Solano, E. Caurier, F. Nowacki, *Nucl. Phys. A* **694**, 157 (2001).
15. D.R. Tilley, C. Cheves, J. Kelley, S. Raman, H. Weller, *Nucl. Phys. A* **636**, 249 (1998).
16. P.M. Endt, *Nucl. Phys. A* **633**, 1 (1998).
17. J.A. Cameron, B. Singh, *Nucl. Data Sheets* **88**, 299 (1999).
18. F. Brandolini *et al.*, *Nucl. Phys. A* **642**, 387 (1998).
19. F. Glatz, P. Betz, J. Siefert, F. Heidinger, H. Röpke, *Phys. Rev. Lett.* **46**, 1559 (1981).
20. M. Dufour, A.P. Zuker, *Phys. Rev. C* **54**, 1641 (1996); A.P. Zuker, J. Retamosa, A. Poves, E. Caurier, *Phys. Rev. C* **52**, R1741 (1995).